Available online at www.sciencedirect.com
SCIENCE DIRECT®
Journal of Chromatography B, 807 (2004) 39–45
JOURNAL OF CHROMATOGRAPHY B
www.elsevier.com/locate/chromb

Surfactant-aided size exclusion chromatography

D.A. Horneman [a], M. Wolbers [a], M. Zomerdijk [a], M. Ottens [a], J.T.F. Keurentjes [b], L.A.M. van der Wielen [a,*]

[a] *Department of Biotechnology, Delft University of Technology, Julianalaan 67, 2628 BC Delft, The Netherlands*
[b] *Process Development Group, Eindhoven University of Technology, P.O. Box 513, 5600 MB, Eindhoven, The Netherlands*

Available online 27 February 2004

Abstract

The flexibility and selectivity of size exclusion chromatography (SEC) for protein purification can be modified by adding non-ionic micelle-forming surfactants to the mobile phase. The micelles exclude proteins from a liquid phase similar to the exclusion effect of the polymer fibers of the size exclusion resin. This surfactant-aided size exclusion chromatography technology (SASEC) is demonstrated on the separation of two model proteins; bovine serum albumin (BSA) and myoglobin (Myo). The effect of the added surfactants on the distribution behavior of the proteins is predicted adequately by a size exclusion model presented in this paper.

Keywords: Micelle-forming surfactants; Bovine serum albumin; Myoglobin

1. Introduction

Biopharmaceutical products such as biomolecules (hormonal peptides, proteins), and bioparticles (vaccines, viral vectors) have to satisfy extreme purity demands. The purification of molecules with a near-identical chemical composition such as multimers from monomeric products, usually requires costly purification and substantial use of auxiliary materials. In the case of multimer-monomer separation, size exclusion column chromatography (SEC) is the method commonly used. The selectivity depends on the extent of exclusion of a certain species from uncharged gel particles. Therefore, the key parameters are the porosity of the gel, the degree of cross-linking and the ratio of the diameters of the species to be separated and the diameter of the pores or fibers in the gel.

Because too large species are fully excluded and too small species can completely penetrate the gel particles, this chromatographic column technique has a limited selectivity and a restricted flexibility, because each specific separation requires a specific gel. This is unfortunate, given the relatively high prices of these gel materials. Another limitation is that once a certain gel material is selected, the efficiency of separation can only be improved by reducing the amount to be purified, decreasing the flow or increasing the column length. This affects the volumetric productivity or the product concentration in a negative manner.

Here, we propose an alternative method based on the integration of *non-selective* size exclusion chromatography (SEC) and a *selective* mobile phase containing micelles of a specific size. The way in which biomolecules and bioparticles partition towards a phase containing “inert” micelles of nonionic surfactants, depends on the same parameters as in gel filtration chromatography: the volume fraction of micelles and the diameter ratio of solute and micelles [1]. The larger component will be excluded to a higher extent from the micellar mobile phase than the smaller component, which will elute first. In theory, the gel matrix should act as a practically non-selective “storage” phase for proteins but selectively exclude micelles. Small species elute first, thereby reversing the “normal” chromatographic behavior (Fig. 1).

The average micellar shape and size, and thus the selectivity of the protein separation, can be tuned in situ by varying the solution conditions, such as concentration and type of surfactants, temperature as well as type and concentration of added salts [2]. The possibility to vary the solution conditions in situ adds another degree of freedom to normal SEC. Further, this flexible selectivity makes this method more suitable for gradient simulated moving bed (SMB) chromatography which uses the gradient in selectivity to improve the performance of the separation method. It has been

* Corresponding author. Tel.: +31-15-27-82342; fax: +31-15-27-82355.
E-mail address: l.a.m.vanderwielen@tnw.tudelft.nl (L.A.M. van der Wielen).

1570-0232/$ – see front matter © 2004 Elsevier B.V. All rights reserved.
doi:10.1016/j.jchromb.2004.01.061

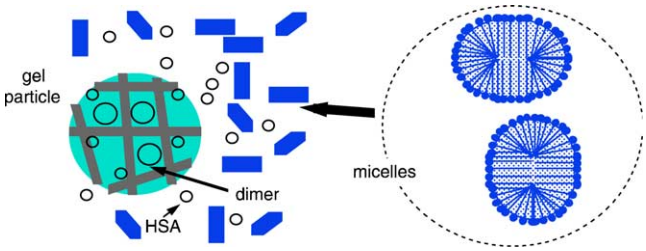

Fig. 1. Schematic representation of selective exclusion of large (in this case multimeric) species from the micellar liquid phase.

shown that gradient SMB can result in lower solvent consumption and less dilution of the product [3]. The analysis of SASEC in SMB technology is not included in this paper.

The separation described here, is based on the excluded volume interactions between the micelles and the proteins and should not be confused with micellar SEC where attractive interactions between the micelles and proteins are used to increase the selectivity [4,5].

The *aim* of this study is to proof the principle of the method described above, and show that micelles can indeed influence the selectivity of size exclusion chromatography. In this paper we will focus on the influence of the concentration of non-ionic surfactants on the distribution coefficient of proteins. Therefore, pulse experiments on fixed bed gel-filtration are performed with the proteins bovine serum albumin (BSA) and myoglobin (Myo) to determine the distribution coefficients of both proteins as a function of surfactant concentration. The surfactants used in this work are non-ionic alkylpolyoxyethylene glycol ethers. These non-ionic surfactants are used to minimize interactions other than size exclusion interactions [6].

Furthermore, a model based on excluded volume interactions is presented to predict the influence of micelles on the distribution behavior of proteins.

2. Theory

2.1. Distribution coefficients in size exclusion chromatography

The elution of a solute i is characterized by its distribution coefficient, K_i, which is defined as the ratio of the solute concentration in the gel phase, $C_{\mathrm{gel},i}$, over the solute concentration in the mobile phase, $C_{\mathrm{mobile},i}$ at equilibrium. Throughout this paper, the gel phase is defined as the total gel volume, including the fibers of the gel particles.

$$K_i = \frac{C_{\mathrm{gel},i}}{C_{\mathrm{mobile},i}} \tag{1}$$

Relatively large solutes cannot diffuse into the pores and have a K-value close to 0, whereas relatively small solutes can diffuse into the pores relatively easily and have higher K-values. K_i can be experimentally evaluated by the determination of the experimental elution volume, V_e of a given solute by means of pulse experiments. The elution volume is then normalized to a column-independent distribution coefficient by [7]:

$$K = \frac{V_e - V_0}{V_t - V_0} \tag{2}$$

where V_0 is the volume of the mobile phase in the column and V_t is the total volume of the column.

The distribution coefficient is an important parameter in size exclusion chromatography. Therefore, many efforts have been undertaken to predict this distribution coefficient from the size and shape of the solute(s) and the size, shape and concentration of the fibers or obstacles [8–14]. One of the first efforts has been undertaken by Ogston [8], who has derived a model for the distribution coefficient that is based on the available space fraction for a rigid spherical solute in a random distribution of long fibers. This model is only valid for low solute concentrations and can be written as:

$$K_i = \exp\left(-\phi_f\left(1 + \frac{r_i}{r_f}\right)^2\right) \tag{3}$$

where ϕ_f is the volume fraction of fibers in the gel particles and r_i and r_f are the radius of the solute i and the gel fiber, respectively. In this model, the overlap of fibers is neglected. Bosma and Wesselingh [14] extend this model by including the overlap of the fibers:

$$K_i = \exp\left(-\ln\left(\frac{1}{1-\phi_f}\right)\left(1 + \frac{r_i}{r_f}\right)^2\right) \tag{4}$$

In many separation processes, more than one single solute and more than one single type of fiber can be present in the system. To describe the steric interactions among these different solutes and fibers, Blankschtein and coworkers [13] developed a generalized excluded volume model. In this model, all volumes excluded to a solute due to the presence of all types of fibers and solutes, including the solute itself, are calculated in each phase. They derived the following general equation:

$$K_i = \exp\left(-\sum_j \gamma_{ij}^{\mathrm{gel}} + \sum_j \gamma_{ij}^{\mathrm{mobile}}\right) \tag{5}$$

where the dimensionless number γ_{ij}^k is the total excluded volume of solute i and a set of objects j per volume of phase k and is defined as:

$$\gamma_{ij}^{\mathrm{gel}} = x_j^{\mathrm{gel}} U_{ij}^{\mathrm{gel}}, \qquad \gamma_{ij}^{\mathrm{mobile}} = x_j^{\mathrm{mobile}} U_{ij}^{\mathrm{mobile}} \tag{6}$$

where x_j^k is the number concentration of component j in phase k (#/m^3) and U_{ij}^k is the excluded volumes between i and j in phase k. The excluded volume of two convex particles can be calculated by the following general expression [9,13]:

$$U_{ij} = V_i + \frac{S_i H_j + S_j H_i}{4\pi} + V_j \tag{7}$$

where V_i, S_i and H_i are the volume, the surface area and the integral of the mean curvature of component i, respectively. With this expression, it is possible to calculate the excluded volume between two convex objects of any shape or size.

The distribution coefficient of a spherical solute in SEC with only one type of fiber can now be calculated using Eqs. (5)–(7). Assuming that the length of the fibers is substantially larger than the fiber radius, i.e. $l_f \gg r_f$, the distribution coefficients becomes:

$$K_s = \exp\left(-\phi_f\left(1+\frac{r_s}{r_f}\right)^2 - (\phi_s^{gel} - \phi_s^{mobile})\left(1+\frac{r_s}{r_s}\right)^3\right) \quad (8)$$

where ϕ_s is the volume fraction of the solute. The first term in the exponent on the right hand side of Eq. (8) describes the steric interactions between the fiber and the protein in the gel phase. The second term describes the steric self-interaction among the protein molecules themselves in the gel and mobile phase. For dilute protein solutions, the second term can be neglected and Eq. (8) equals the well-known Ogston relation (Eq. (3)).

2.2. Surfactant-aided size exclusion chromatography

To describe the retention behavior of a single protein in surfactant-aided SEC (SASEC), three components are present: the protein (1), the fiber (2) and the micelle (3). Only the micelles and the protein can be present in both phases (gel phase and mobile phase). Using Eq. (5), the distribution coefficient of the protein now becomes:

$$K_1 = \exp(-\gamma_{11}^{gel} - \gamma_{12}^{gel} - \gamma_{13}^{gel} + \gamma_{11}^{mobile} + \gamma_{13}^{mobile}) \quad (9)$$

For dilute protein solutions, the parameters γ_{11}^{gel} and γ_{11}^{mobile} can be neglected because the excluded volume due to the presence of protein molecules is relatively small compared to the total accessible volume. To calculate the excluded volume for proteins due to the presence of micelles, the size and shape of the micelles has to be known. This can be predicted by using a molecular-thermodynamic model of micellization [15,16]. Puvvada and Blankschtein only studied alkylpolyoxyethylene glycol ethers with a relatively short polyoxyethylene chain as the hydrophilic head group and regarded this as a compact head group. This approach does not give satisfactory results with respect to the size prediction when the polyoxy-ethylene chain consists of more than eight oxy-ethylene units. For these large polyoxyethylene chain lengths, the head group is regarded as a polymeric chain [15]. The micelle is then modeled as a hydrophobic core surrounded by a corona: a polymer solution consisting of polyoxyethylene chains (Fig. 2). Both models predict micelles formed by the surfactants used in this study ($C_{12}E_{23}$ and $C_{16}E_{20}$) to be globular and not cylindrical. For spherical micelles, the radius of the micelles is taken as the sum of the radius of the hydrophobic core and the thickness of the hydrophilic corona. The radius of the hydrophobic core can be estimated from the hydrocarbon chain length of the surfactant. The extended hydrocarbon tail length is the maximum possible length of the chain and can be calculated by [17]:

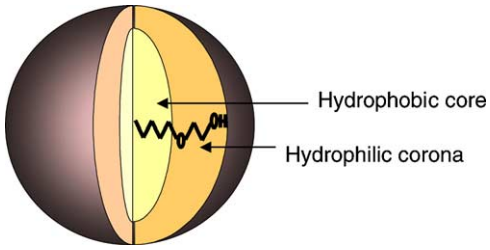

Fig. 2. Schematic representation of a spherical micelle with a hydrophobic core and a hydrophilic corona.

$$l_{max} = 1.5 + 1.265(n_c - 1) \quad (10)$$

where n_c is the number of carbon atoms in the hydrocarbon chain. Hydrocarbon chains in the liquid state are not fully extended and thus the hydrocarbon tail length is always smaller than the extended tail length. For $C_{12}E_{23}$ the hydrocarbon tail length is estimated to be about 75% of the extended hydrocarbon tail length [17,18] and for $C_{16}E_{20}$ the length is estimated to be about 62% of the extended hydrocarbon tail length [18].

In this study, the thickness of the hydrophilic corona is taken from the simulation results of Nagarajan [15], which corresponds with experimental work of Tanford [18]. From the study of Tanford can be deduced that the hydrophobic core cannot be a perfect sphere when the micelles are formed by one of the two surfactants used in this study, as there is simply not enough space in the spherical core to contain all the hydrophobic tails [18]. Therefore, the hydrophobic core must have an oblate shape. An oblate micelle is defined by three semi-axes r_m, r_m and $\eta_m r_m$ where $\eta_m < 1$. The semi-axes r_m and $\eta_m r_m$ are assumed to be 4.13 and 3.66 nm for $C_{12}E_{23}$ and 4.69 and 3.77 nm for $C_{16}E_{20}$ [17]. The distribution coefficient of a spherical solute (dilute solution) now becomes [9,13]:

$$K_s = \exp\left(-\ln\left(\frac{1}{1-\phi_f}\right)\left(1+\frac{r_s}{r_f}\right)^2 - (\phi_m^{gel} - \phi_m^{mobile}) \times \left(1+\frac{1}{\eta_m}\left(\frac{r_s}{r_m}\right)^3 + \frac{3}{2}\left(\frac{r_s}{r_m}\right)^2\frac{g(\eta_m)}{\eta_m} + \frac{3}{2}\left(\frac{r_s}{r_m}\right)\frac{f(\eta_m)}{\eta_m}\right)\right) \quad (11)$$

$$f(\eta_i) = 1 + \eta_i^2(1-\eta_i^2)^{-1/2}\cosh^{-1}(\eta_i^{-1})$$

$$g(\eta_i) = \eta_i + (1-\eta_i^2)^{-1/2}\cos^{-1}(\eta_i^{-1})$$

3. Materials and method

3.1. Equipment

The pulse experiments were performed on an FPLC system, controlled by Unicorn version 2.01 (Amersham Pharmacia Biotech Benelux). The concentration of the proteins in the outlet of the column was determined on-line by a spectrophotometer at two different wavelengths (280 and 405 nm). During the break-through experiments, the concentration of the surfactants was measured on-line at 206 nm. The density of the eluent was also determined in all experiments.

3.2. Column

An XK16 column from Pharmacia Biotech was used in the system. The column was packed with Sephacryl™ S300 HR (Amersham Biosciences BV, cat no. 17-0599-01) up to a height of 7 cm. The volume fraction of the gel fibers, ϕ_f, has been determined with salt pulses. Small salt molecules (NaCl) can diffuse into all the pores of the gel. The difference between the elution volume of NaCl and the geometrical volume of the column gives the volume of the gel fibers. A value of 0.08 was found for this gel, the radius of the gel fiber, r_f was assumed to be 15 nm. This assumption has been made by fitting known distribution coefficients of calibration proteins (data provided by Amersham Pharmacia Biotech) to the Ogston equation (Eq. (4)). The dead volume of the system (total volume between injection point and spectrophotometer minus the column volume itself) is determined by pulses of dextran blue and BSA. The void volume of the packed column is determined by dextran blue pulses.

3.3. Experiments

Pulses of 0.5 ml containing 10 g/l BSA (Sigma, cat no. A 7906) or 1.5 g/l Myo from horse heart (Sigma cat no. M18882 >90% pure) in a surfactant-buffer solution were injected. In all experiments, a 10 mM phosphate buffer, pH 6.8 containing 0.1 M NaCl and a known concentration of surfactant was used as eluent. The surfactants used in these experiments were the non-ionic surfactants $C_{12}E_{23}$ (Acros organics, cat no. 228345000) and $C_{16}E_{20}$ (Acros organics, cat no. 344295000). Various surfactant concentrations between 0 and 20 wt.% were used in the eluent. In order to determine the distribution coefficient of the surfactants, break-through curves of the surfactants were measured at the different surfactant concentrations.

4. Results and discussion

4.1. Distribution coefficients of BSA and Myo as function of surfactant concentration; experimental results

The pulse response curves already show the effect of the presence of micelles on the elution behavior of the proteins.

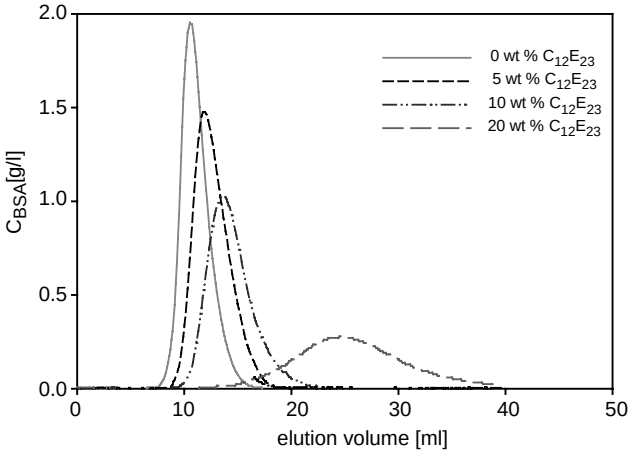

Fig. 3. Pulse response curves of BSA at different concentrations of $C_{12}E_{23}$. $C_{BSA,feed} = 10$ g/l, pulse volume = 0.5 ml.

Fig. 3 shows some examples of the pulse response curves measured in the BSA-$C_{12}E_{23}$ systems. As expected, it shows an increase in elution volume of BSA with increasing surfactant concentration. From these measured pulse response curves the distribution coefficients of the protein have been determined, using Eq. (2), where the elution volume is the volume corresponding to the peak of the pulse response curve. The elution volume and the void volume are both corrected for the dead volume of the system. The results of these calculations can be seen in Fig. 4, which shows the distribution coefficient as function of the surfactant concentration. The protein distribution coefficient increases with increasing surfactant concentration, which indicates that the proteins are indeed excluded to a higher extent from the

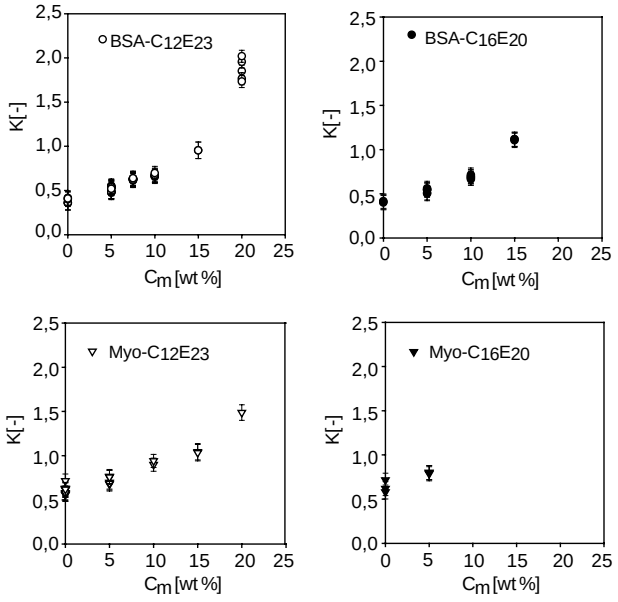

Fig. 4. Distribution coefficients of BSA (circles) and myoglobin (triangles) as function of surfactant concentration, for the two tested surfactants $C_{12}E_{23}$ and $C_{16}E_{20}$.

mobile phase into the gel phase at higher surfactant concentration. The micelles formed by the two different surfactants, $C_{12}E_{23}$ and $C_{16}E_{20,}$ have about the same size and shape but differ in hydrophobicity. Fig. 4 shows that there is no significant difference in distribution coefficients of the proteins between the two different surfactant-gel systems. This indicates that the effect on the distribution coefficient is indeed mainly determined by the size and shape of the micelle.

Fig. 4 also shows that in this case a selective gel has been used. The distribution coefficients of BSA and Myo at 0 wt.% of surfactant is less than unity and BSA has a smaller distribution coefficient than Myo. Increasing the surfactant concentration has, however, a larger influence on the distribution coefficient of BSA than of Myo. The distribution coefficient of BSA changes from 0.39 at 0 wt.% up to 2 at a concentration of 20 wt.% of $C_{12}E_{23}$, while the distribution coefficient of Myo only changes from 0.6 up to 1.5 in the same concentration range. This difference of influence on two different sized proteins proves that changing the surfactant concentration in the mobile phase can change the selectivity of SEC. The ability to change the selectivity in situ, improves the flexibility of this separation method.

The data further shows that introducing micelles in the mobile phase increases the distribution coefficients of the proteins beyond the normal range found in SEC, i.e. between 0 and 1. Values of K_{BSA} up to 2 can be achieved at a concentration of 20 wt.% of $C_{12}E_{23}$.

4.2. Distribution coefficients of the micelles, experimental and model results

The distribution of the micelles into the gel phase has to be known before any prediction can be made of the distribution coefficient of the proteins. Fig. 5 shows the experimentally determined distribution coefficients of the surfactants. It shows an increase in *K*-values at increasing surfactant concentration. Thus also the micelles themselves are more excluded from the mobile phase into the gel-phase at higher surfactant concentrations. Using Eqs. (5)–(7), the distribution coefficients of the micelles can be predicted. To do so, all experimentally determined weight fractions were recalculated to volume fractions by:

$$\phi_{in} = \frac{w_{in}\rho N_{av}}{M_w N} V_m \quad (12)$$

where w_{in} is the mass fraction of the micelles in the eluent, ρ the density of eluent, M_w the molar mass of one surfactant molecules, N the aggregation number of the micelle (the number of surfactant molecules per micelle) and V_m is the volume of a micelle. The aggregation number of $C_{12}E_{23}$ and $C_{16}E_{20}$ are 50 and 70, respectively [15].

The model prediction (Eqs. (5)–(7)) of the distribution coefficients is represented as a line in Fig. 5. The model prediction is in good agreement with the experimentally determined distribution coefficients of the surfactants and is therefore used in the further calculations.

4.3. Distribution coefficients of the proteins as function of surfactant concentration; modeling results

Eq. (11) is now used to predict the distribution coefficient of BSA and Myo as function of the concentration of surfactant in the mobile phase. Figs. 6 and 7 compare the predicted *K*-values with the average of the experimentally found *K*-values using $C_{16}E_{20}$ and $C_{12}E_{23}$ as surfactant. Up to a concentration of 10 wt.% of surfactant in the mobile phase, the model predictions are in good agreement with the experimental results. At higher concentrations, the model predicts that the distribution coefficient of the proteins is becoming almost constant, while the experimental data show a further increase of the distribution coefficients at higher concentrations of surfactant.

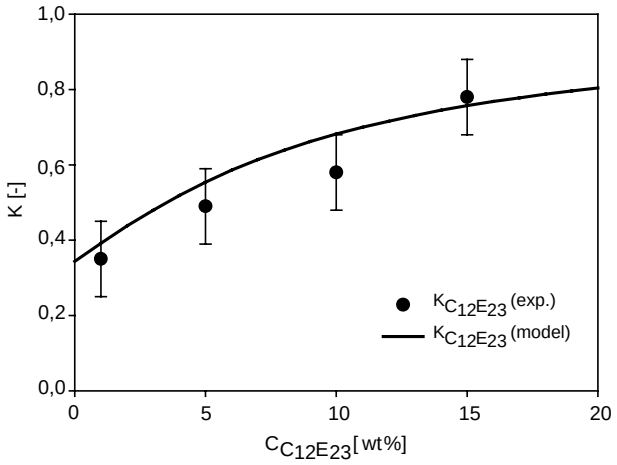

Fig. 5. Comparison between the model predictions of the distribution coefficient of $C_{12}E_{23}$ the experimentally found values as function of the concentration of $C_{12}E_{23}$.

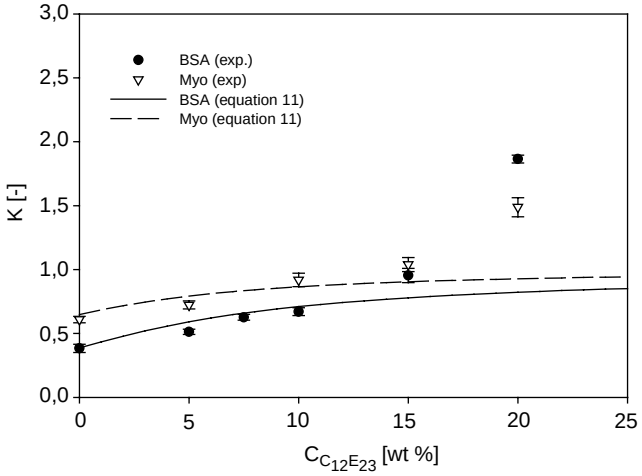

Fig. 6. Comparison between the model predictions of the distribution coefficients of BSA and Myo using Eq. (11) and the average of the experimentally found *K*-values for BSA and Myo as function of the concentration of $C_{12}E_{23}$.

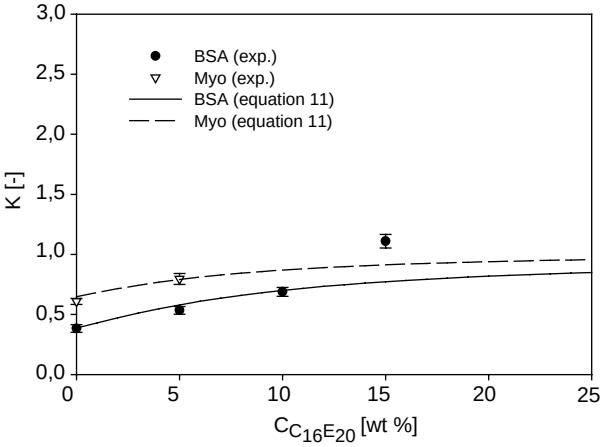

Fig. 7. Comparison between the model predictions of the distribution coefficients of BSA and Myo using Eq. (11) and the average of the experimentally found *K*-values for BSA and Myo as function of the concentration of $C_{16}E_{20}$.

The model described by Eq. (11) does not take into account the possible overlap of the micelles at high concentrations. The excluded volume for the proteins, due to the presence of the micelles, will be underestimated by this model. The distribution coefficient of micelles levels off (Fig. 5), which means that the concentration ratio of the micelles in the mobile and the solid phase becomes constant. The concentration difference between the two phases thus increases with increasing surfactant concentration. This will cause a higher driving force and the protein will distribute more into the solid phase, than predicted without fiber overlap.

At low surfactant concentrations this overlap can be neglected but at higher concentrations the overlap will influence the distribution behavior of the other solutes (Lazarra, Blankschtein and Deen, 2000). In the same way as the original Ogston relation was extended for fiber overlap, the model described here can be extended for the overlap of the micelles (Bosma and Wesselingh, 2000; Lazarra, Blankschtein and Deen, 2000): Eq. (11) than becomes:

$$K_s = \exp\left(-\ln\left(\frac{1}{1-\phi_f}\right)\left(1+\frac{r_s}{r_f}\right)^2 - \left(\ln\left(\frac{1}{1-\phi_m^{gel}}\right) - \ln\left(\frac{1}{1-\phi_m^{mobile}}\right)\right)\left(1+\frac{1}{\eta_m}\left(\frac{r_s}{r_m}\right)^3 + \frac{3}{2}\left(\frac{r_s}{r_m}\right)^2\frac{g(\eta_m)}{\eta_m} + \frac{3}{2}\left(\frac{r_s}{r_m}\right)\frac{f(\eta_m)}{\eta_m}\right)\right) \quad (13)$$

Figs. 8 and 9 compare the results of Eq. (13) with the experimental data. The prediction of the distribution coefficient of BSA and Myo is now in good agreement with the experimental results. Even better results may be achieved when other interactions between the micelles and proteins are incorporated in the model besides the steric interactions. The associated increase in model complexity should be balanced against the increase in model accuracy.

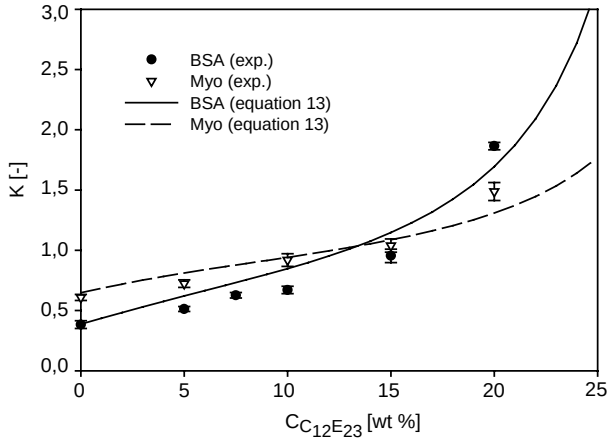

Fig. 8. Comparison between the model predictions of the distribution coefficients of BSA and Myo using Eq. (13) and the average experimentally found *K*-values for BSA and Myo as function of the concentration of $C_{12}E_{23}$.

4.4. Future outlook

The case described in this paper shows the ability to change the selectivity in-situ by using SASEC. Using the chosen combination of gel and surfactant for the separation of BSA and Myo is probably not the best choice for applying this SASEC method in fixed bed chromatography. The gel is still selective, which means that first a certain threshold concentration of surfactant should be reached before improvement of the selectivity will occur. Fig. 4 shows that at about 15 wt.% the elution behavior of normal SEC is reversed. At higher surfactant concentrations the selectivity will improve. To improve the selectivity at lower surfactant concentrations ($\phi_m^{gel} - \phi_m^{mobile}$) should be increased and/or r_m should be decreased (see Eq. (13)). This is possible by using for example long cylindrical micelles with a small diameter.

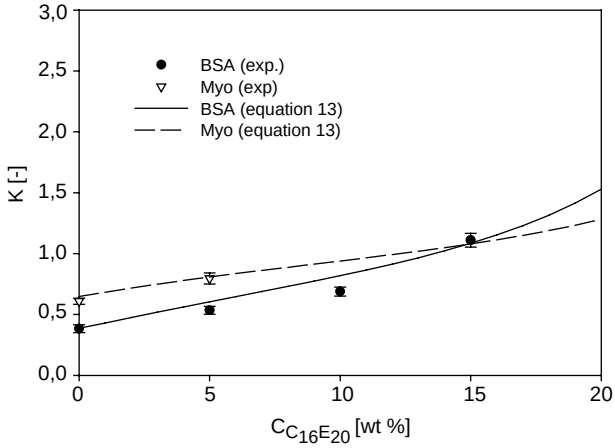

Fig. 9. Comparison between the model predictions of the distribution coefficients of BSA and Myo using Eq. (13) and the average experimentally found *K*-values for BSA and Myo as function of the concentration of $C_{16}E_{20}$.

Long cylindrical micelles will have a lower distribution towards the solid phase compared to spherical micelles. This will results in a higher values for $(\phi_m^{gel} - \phi_m^{mobile})$.

An improvement of selectivity is not even necessary when gradient simulated moving bed chromatography (gradient-SMB) is used [3,19]. Normal SMB can already reduce resin and eluent consumption and maintain a high product concentration at the same time. With gradient-SMB the resin and eluent consumption can be further reduced and even more concentrated products can be reached. Another advantage of using SMB-chromatography is that the surfactants can be separated from the product in the same unit operation, if necessary (this doesn't have to be necessary as some surfactants are being used in industrial practice to formulate the end product).

5. Conclusions

The elution time, and thus the distribution coefficient of a protein, during size exclusion chromatography is increased by using nonionic surfactants above their CMC in the mobile phase. This increase is different for proteins of different sizes, what implies that changing the surfactant concentration in the mobile phase changes the selectivity of the separation in-situ. The ability of changing the selectivity makes SASEC more flexible than the conventional SEC for protein purification and will probably decrease the size of SEC equipment and reduce the eluent consumption.

The model presented in this paper is based solely on the excluded volume interactions between the proteins, micelles and the fibers. It does describe qualitatively the influence of non-ionic micelle-forming surfactant on the distribution of proteins. An even more accurate description of the behavior may be achieved when other interactions between the micelles and proteins are incorporated in the model besides the steric interactions. The associated increase in model complexity should be balanced against the increase in model accuracy.

6. Nomenclature

C_i^k	concentration of solute i in phase k
K_i	distribution coefficient of component i
l_{max}	extended hydrophobic tail length
M_i	integral of mean curvature of component
n_c	number carbon atoms in hydrocarbon tail
N	Avogadro number
N_{av}	aggregation number
r_i	radius of component i
S	selectivity
S_i	surface area of component i
U_{ij}	excluded volume between components i and j
V_e	elution volume
V_i	volume of component i
V_o	void volume
V_t	total volume of column
x_i	number concentration of component i

Greek letters

γ_{ij}	steric interaction parameter between components i and j
ρ	density
ϕ_i	volume fraction of component i

Subscripts

f	gel fiber
gel	gel phase
m	micelle
mobile	mobile phase
s	solute

Superscripts

gel	gel phase
mobile	mobile phase

References

[1] C. Liu, D.T. Kamei, J.A. King, D.I. C Wang, D. Blankschtein, J. Chromatogr. B711 (1998) 127.
[2] D.F. Evans, H. Wennerström, The Colloidal Domain, VCH, New York, 1994.
[3] T.B. Jensen, T.G.P. Reijns, H.A.H. Billiet, L.A.M. van der Wielen, J. Chromatogr. A873 (2000) 149.
[4] D.G. Herries, W. Bishop, F.M. Richards, J. Phys. Chem. 68 (1968) 1843.
[5] A. Berthod, C. Garcia-Alvarez_Coque, Micellar Liquid Chromatography, Chromatographic Science Series 83, Dekker, New York, 2000.
[6] Y.J. Nikas, C. Liu, T. Srivastava, N.L. Abbot, D. Blankschtein, Macromolecules 25 (1992) 4797.
[7] L. Fisher, Gel Filtration Chromatography, Elsevier/North-Holland, Amsterdam, 1980.
[8] G. Ogston, Trans. Faraday Soc. 54 (1958) 1754.
[9] K.M. Jansons, C.G. Phillips, J. Colloid Interface Sci. 137 (1989) 75.
[10] L.A. Fanti, E.D. Glandt, J. Colloid Interface Sci. 135 (1990) 385.
[11] E.M. Johnson, W.M. Deen, J. Colloid Interface Sci. 178 (1996) 749.
[12] P.R. Wills, Y. Georgalis, J. Dijk, D.J. Winzor, Biophys. Chem. 57 (1995) 37.
[13] M.J. Lazzara, D. Blankschtein, W.M. Deen, J. Colloid Interface Sci. 226 (2000) 112.
[14] J.C. Bosma, J.A. Wesselingh, J. Chromatogr. B 743 (2000) 169.
[15] R. Nagarajan, E. Ruckenstein, Langmuir 7 (1991) 2934.
[16] S. Puvvada, D. Blankschtein, J. Chem. Phys. 92 (1990) 3710.
[17] C. Tanford, The Hydrophobic Effect Formation of Micelles and Biological Membranes, Wiley, New York, 1980.
[18] C. Tanford, Y. Nozaki, M.F. Rhode, J. Phys. Chem. 81 (1977) 1555.
[19] J. Houwing, H.A.H. Billiet, L.A.M. van der Wielen, AIChE J. 49 (2003) 665.